H. X. Pei, M. W. Brown,† and K. J. Miller†*

Fatigue Crack Propagation under Complex Biaxial Stress Cycling

REFERENCE Pei, H. X., Brown, M. W., and Miller, K. J., **Fatigue crack propagation under complex biaxial stress cycling**, *Biaxial and Multiaxial Fatigue*, EGF 3 (Edited by M. W. Brown and K. J. Miller), 1989, Mechanical Engineering Publications, London, pp. 587–603.

ABSTRACT An experimental study of Mode I fatigue crack growth under complex biaxial loading has been carried out over a wide range of cyclic stress levels and waveforms at room temperature. A simple approach is proposed for correlating crack propagation rate. The results emphasize the contribution of plasticity to fatigue crack growth and indicate a relationship between uniaxial fracture mechanics parameters, and the biaxial crack propagation rate.

Introduction

Many engineering structures and machine parts are subjected to repeated loadings, which may lead to their failure due to fatigue. It is frequently recognized that, for most in-service structures and components, the stressing system is not a simple uniaxial one. Biaxial and triaxial stress states can often exist, where the components of stress may be either in-phase or out-of-phase with one another.

Multiaxial fatigue has been studied for a number of years and the results of experimental and theoretical work have been related to many criteria. Attention is drawn to reviews by Brown and Miller (**1**) and Garud (**2**). These two reviews deal mainly with proportional loading, but non-proportional (i.e., out-of-phase) loading is also of significance because of the not infrequent necessity of designing against fatigue under such situations. Non-proportional loading experiments can also assist our basic understanding of crack extension processes. Presently, experimental data from non-proportional loading tests are very limited and are briefly reviewed elsewhere (**3**)(**4**).

In order to obtain fundamental information on crack propagation behaviour, an experimental room temperature study of Mode I fatigue crack growth has been carried out using complex biaxial stress waveforms over a wide range of cyclic stress levels. The results emphasize the importance of plasticity in fatigue crack growth and indicate a good correlation between elastic–plastic fracture mechanics parameters and the crack propagation rate.

* The Institute of Metal Research, Academia Sinica, Shenyang, China.
† University of Sheffield, Department of Mechanical Engineering, Mappin Street, Sheffield S1 3JD, UK.

Notation

A	Constant
a	Half crack length
a_o, a_f	Initial and final crack lengths respectively.
c	Constant
E	Young's modulus
F	Stress intensity geometry factor
J	Contour integral
K	Stress intensity factor
m, n	Constants
N_f	Number of cycles to failure
R	Stress ratio $\sigma_{min}/\sigma_{max}$
w	Half specimen width
W_e, W_p, W_t	Elastic, plastic and total strain energy densities, respectively
x, y	Cartesian coordinates
X	Modified strain energy density function
α	Strain hardening exponent
Δ	Range
δ(CTOD)	Crack tip opening displacement
$\varepsilon_e, \varepsilon_p, \varepsilon_t$	Elastic, plastic, and total strains, respectively
λ	Ratio of stress amplitudes (σ_2/σ_1)
ν	Poisson's ratio
σ	Normal stress
$\sigma_1, \sigma_2, \sigma_3$	Principal stresses $(\sigma_1 \geq \sigma_2 \geq \sigma_3)$
σ_T	Flow stress
σ_y	Yield stress
σ_v	von Mises type stress
σ_{eff}	Effective stress
ϕ	Phase difference

Elastic–plastic parameters for uniaxial Mode I crack growth

Linear elastic-fracture mechanics (LEFM) has been used to correlate fatigue crack growth rate for several years. The stress intensity factor, K, has commonly been accepted for describing crack growth under small scale yielding (SSY) conditions. However, the strict SSY limitations are exceeded when stress levels approach general yielding. Thus a number of alternative fracture mechanics parameters have been proposed for studying crack growth at high stress levels, some common examples being ΔJ, the cyclic contour integral (**5**)(**6**), the crack-tip opening displacement (**7**), and the cyclic plastic zone size (**8**); all three of which are reviewed in reference (**9**).

Cai (**10**) has used an expression for uniaxial stress cycling based on the monotonic stress-strain relationship and which can be expressed as

$$P = 2\pi F^2 a \int \sigma \, d\varepsilon \tag{1}$$

where F is a geometric factor which under LEFM conditions is equivalent to $K/\{\sigma\sqrt{(\pi a)}\}$.

In this paper the term P is used instead of J since the latter term is essentially a non-linear elastic parameter, while P is a more general elastic–plastic parameter. It follows that when calculating $\int \sigma \, d\varepsilon$ in equation (1), both the linear elastic and the power-law hardening plastic components may be evaluated separately, and then combined to give the more general elastic–plastic Ramberg–Osgood type of stress–strain behaviour. The stable cyclic stress–strain curve generally deviates smoothly from the elastic line, so that an equation of the following form usually fits the data

$$\varepsilon_t = \varepsilon_e + \varepsilon_p = \frac{\sigma}{E} + \left(\frac{\sigma}{A}\right)^{1/\alpha} \tag{2}$$

Figure 1 illustrates the quantities ε_t, ε_e, ε_p, and σ.

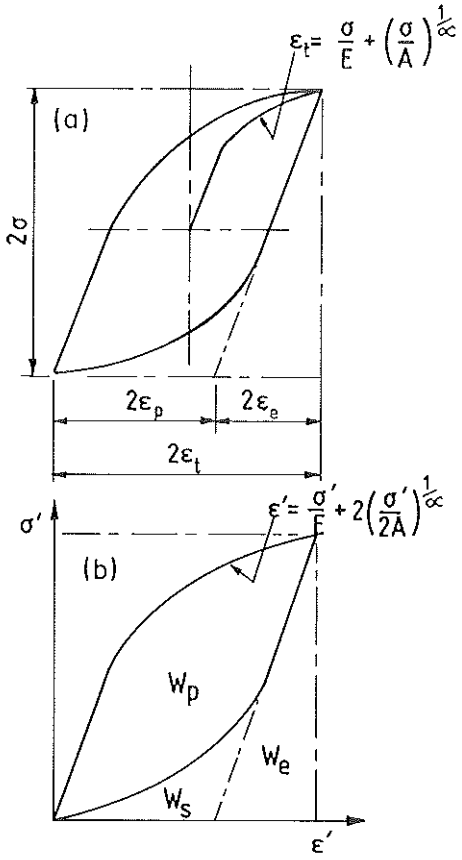

Fig 1 Hysteresis loop for fully reversed loading: (a) defining cyclic stress strain curve; (b) defining components of strain energy

Re-arranging the second term of equation (2), one obtains the power law hardening equation

$$\sigma = A\varepsilon_p^{\alpha} \tag{3}$$

In the case of fatigue loading, a cyclic term ΔP can be evaluated by considering the elastic and plastic components

$$\Delta P = \Delta P_e + \Delta P_p = 2\pi F^2 a \int_0^{\Delta\varepsilon} \sigma' \, d\varepsilon' \tag{4}$$

where σ' and ε' are defined in Fig. 1(b).

For simplicity, the stable hysteresis loop has been defined by the cyclic stress–strain curve, although this curve does not necessarily provide complete information about the shape of the hysteresis loop. Dowling (**11**) showed that agreement between the stabilized hysteresis loop traces and the expanded cyclic stress–strain curve was almost perfect for the one example of 2024-T4 aluminium, but such behaviour can also be observed in a range of materials, though not in every case (**12**). From a knowledge of the hysteresis loop shape, expressions can be derived for the energy absorbed per cycle per unit volume of material (see Appendix 1).

In equation (4) the integral $\int \sigma' \, d\varepsilon'$ should be evaluated only over the period of the cycle where the crack is open. For fully reversed load cycling ($R = -1$), see Fig. 1(a), the crack opening load should lie between the point of load reversal and zero load (**9**) for plane strain conditions, hence the value of ΔP should lie between the following two terms (see Appendix 1)

$$\Delta P_A = 2\pi F^2 a\{W_e + W_p/(1 - \alpha)\} \tag{5}$$

and

$$\Delta P_B = 2\pi F^2 a(W_e + 2W_p)/4 \tag{6}$$

although ΔP will probably be closer to ΔP_B (**9**).

For repeated loading ($R = 0$) and plane strain conditions, there appears to be no significant crack closure. In experiments at high stress levels (**9**) oxide was unable to build up due to the fast crack propagation rate for the case of a stainless steel. The effect of surface roughness was also assessed by examination in the scanning electron microscope to show that roughness-induced closure was negligible. Therefore, one may take

$$\Delta P_C = 2\pi F^2 a\{W_e + W_p/(1 - \alpha)\} \tag{7}$$

for this loading mode.

Based on the strip yield model of crack tip plasticity, Tomkins (**7**) has extended the CTOD approach to fatigue crack propagation to include the plastic strain range contribution. For a crack loaded in tension, in an infinite plate, the CTOD is given by

$$\delta = \frac{\pi\sigma^2}{2\sigma_T E}\, a + \frac{\pi\sigma\Delta\varepsilon_p}{\sigma_T(1+\alpha)}\, a \tag{8}$$

for small values of α and $\sigma/\sigma_T < 0.5$. Equation (8) may be rephrased in terms of the elastic and plastic energy components, to give

$$\delta = \frac{\pi a}{\sigma_T}\{W_e + 2W_p/(1-\alpha)\}/4 \tag{9}$$

Now δ is proportional to the non-linear elastic parameter J which is frequently identified as being equal to $m\sigma_y\delta$. This can be translated to

$$\begin{aligned}\Delta P_D &= m\sigma_T\delta \\ &= m\pi a\{W_e + 2W_p/(1-\alpha)\}/4\end{aligned} \tag{10}$$

where m is usually taken to be equal to 2.

Comparison of equations (5), (6), (7), and (10) shows that ΔP may always be represented by an equation of the general form

$$\Delta P = 2\pi F^2 a(W_e + DW_p)B \tag{11}$$

where D and B are constants. Irrespective of the assumptions made concerning crack closure, the value of D does not vary by more than a factor of 2, since

$$1/(1-\alpha) \leq D \leq 2/(1-\alpha) \tag{12}$$

Other examples of values for D may be found in the literature (**5**)(**6**). An important three-dimensional example is the thumbnail crack initiated on the surface of a uniaxially loaded low cycle fatigue specimen (6) where, for the case of no crack closure

$$\Delta P_E = 3.2a\{W_e + 1.56W_p/(1-\alpha)\} \tag{13}$$

which also conforms with equations (11) and (12).

Parameters for biaxial cyclic stress state

The concept of an equivalent stress is frequently applied to the analysis of biaxial and multiaxial loading situations, and for most metallic materials the von Mises and Tresca criteria are widely used for computing the extent of plasticity.

For an equibiaxial stress of magnitude σ ($\sigma_1 = \sigma_2$, $\sigma_3 = 0$) the equivalent von Mises stress is given by

$$\sigma_v = \sqrt{\{(\sigma_1-\sigma_2)^2 + (\sigma_2-\sigma_3)^2 + (\sigma_3-\sigma_1)^2\}/2} = \sigma \tag{14}$$

while for a uniaxial stress of the same magnitude, σ_v is also equal to the applied stress σ. However, it is known that a direct stress applied on a plane perpendicular to a crack will influence crack tip plasticity (**13**), whereas the von Mises

criterion is only used for an uncracked isotropic material. When material contains a defect or crack, it will exhibit 'anisotropic' behaviour, in so far that the effect of σ_1, the stress normal to the crack, will be different under biaxially loaded systems than that predicted by the von Mises criterion.

It is, therefore, proposed that a fatigue crack growth correlation for the biaxial stress case should incorporate a biaxial stress function that depends on both plastic flow and the stress normal to the crack. Since biaxial constraints develop stresses proportional to Poisson's ratio, ν, the function required should also depend on ν. This can be seen in the Tomkins crack propagation theory (7), where the essential ingredients are the stress, which determines the extent of crack tip plasticity, and the strain range normal to the crack. The normal strain for elastic conditions is

$$\varepsilon_1 = \frac{1}{E}(\sigma_1 - \nu\sigma_2 - \nu\sigma_3) \tag{15}$$

In an attempt to derive an empirical formula for a fatigue effective stress, equations (14) and (15) need to be reconsidered by employing a term such as

$$\sigma_{\text{eff}} = \sqrt{\{(\sigma_1 - \nu\sigma_2)^2 + (\sigma_1 - \nu\sigma_3)^2 + (\nu\sigma_2 - \nu\sigma_3)^2\}}/\sqrt{2} \tag{16}$$

in which σ_2 and σ_3 are modified by the elastic Poisson's ratio. Here σ_{eff} is an effective stress equivalent to the special case of uniaxial loading normal to the crack. Note equation (16) can only be used for fatigue in which it is required to combine aspects of plastic deformation and fracture mechanics.

For uniaxial loading, σ_{eff} is equal to σ_1 only if the stress is perpendicular to the crack. For equibiaxial loads

$$\sigma_{\text{eff}} = \sigma\sqrt{(1 - \nu + \nu^2)} \tag{17}$$

and for pure shear

$$\sigma_{\text{eff}} = \sigma\sqrt{(1 + \nu + \nu^2)} \tag{18}$$

When there is a phase difference ϕ between σ_1 and σ_2, then for a sinusoidal waveform

$$\sigma_1 = \sigma \sin(\omega t) \tag{19}$$

and

$$\sigma_2 = \lambda\sigma \sin(\omega t + \phi) \tag{20}$$

whence

$$\sigma_{\text{eff}} = \sigma\sqrt{\{\sin^2(\omega t) - \nu\lambda \sin(\omega t) \sin(\omega t + \phi) + \nu^2\lambda^2 \sin^2(\omega t + \phi)\}} \tag{21}$$

The effective stress for crack propagation in a cycle is the maximum value obtained from equation (21).

For comparative purposes, it is noted that the elastic parameter ΔJ is widely used for uniaxial fatigue tests to correlate crack growth rate da/dN under cyclic plasticity conditions. For biaxial loading, a simple formula for the ΔJ integral has not yet been derived. However, we may use the uniaxial form of the ΔP approach and the effective stress $\Delta\sigma_{\text{eff}}$ to study biaxial stress cases. Thus, a new parameter is proposed, i.e.

$$\Delta P = 2\pi F^2 a(X_e + DX_p)B \tag{22}$$

where D and B are constants given by equation (11), and

$$\begin{aligned} X_e &= \Delta\sigma_{\text{eff}}^2/2E \\ X_p &= 2\Delta\sigma_{\text{eff}}(\Delta\sigma_{\text{eff}}/2A)^{1/\alpha}(1 - \alpha)/(1 + \alpha) \end{aligned} \tag{23}$$

where $\Delta\sigma_{\text{eff}}$ is derived from equation (21), and A and α are taken from the uniaxial cyclic stress–strain curve.

Clearly, X_e and X_p are equal to W_e and W_p for the uniaxial test only.

Experimental procedure

All tests were conducted on AISI 316 austenitic stainless steel taken from one heat. The tensile properties of the material at room temperature are 0.2 per cent proof stress 395 MPa, tensile strength 611 MPa, reduction in area 71 per cent, elongation 57 per cent, Young's modulus of elasticity 198 GPa, and Poisson's ratio 0.29, for the chemical composition (% wt) of 0.06 C, 1.88 Mn, 0.023 P, 0.020 S, 0.62 Si, 17.30 Cr, 13.40 Ni, 2.34 Mo, balance Fe. The material was solution treated at 1070°C and water quenched to give a grain diameter of 52 μm.

Fatigue tests were performed on a Mayes servo-hydraulic biaxial test facility. A tensile/compressive load could be applied to each pair of arms of a cruciform specimen (Fig. 2), thereby developing a biaxial stress field in the working section. Full details of the testing system and specimen design are given in reference (**14**).

The load waveforms used were triangular and all the details of the stress levels, and specimen numbers associated with a particular waveform, are given in Fig. 3; here σ_1 is the applied stress normal to the mode I fatigue crack, and σ_2 the stress parallel to the crack. Crack length measurements were obtained by a d.c. potential drop method and a travelling microscope. The crack length data measured by both methods were the same. Crack growth rates were determined by a least squares fit of a parabola to groups of five crack length readings differentiated to give the crack extension per cycle.

The strains were monitored continuously with two extensometers, for the y axis and x axis, respectively, and the cyclic stress strain hysteresis loops were recorded at intervals (Fig. 4). Here the y axis was normal to the crack plane.

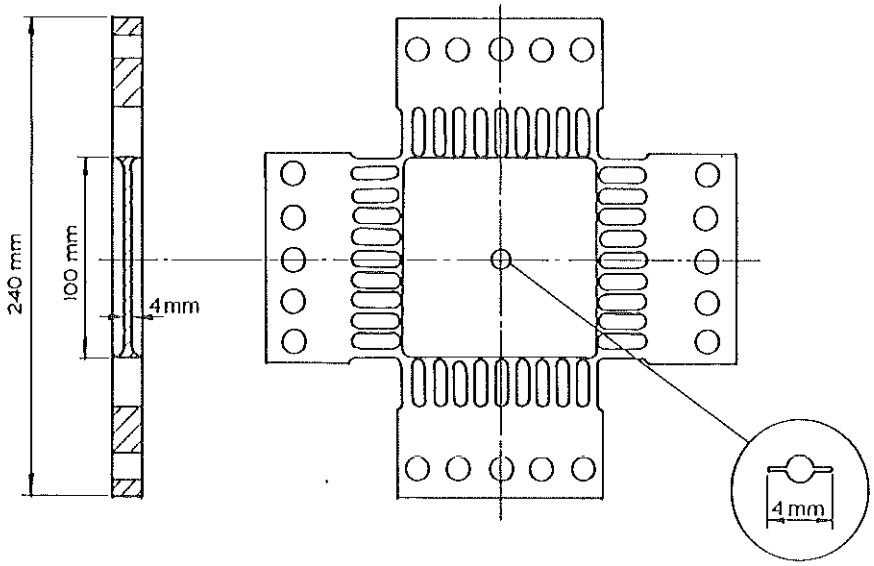

Fig 2 Biaxial fatigue specimen geometry

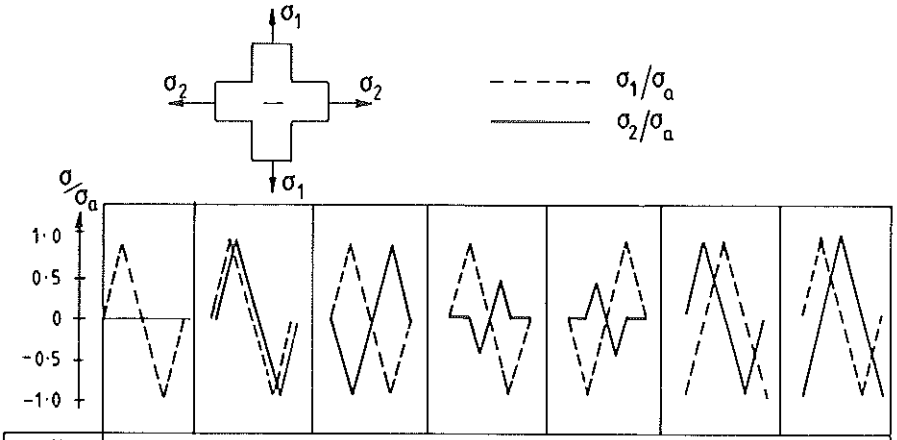

$2\sigma_a$/MPa	SPECIMEN NUMBER						
560	P15	P25	—	P45	P55	P65	P75
386	P13	P23	P33	P43	—	P63	P73
193	P11	P21	P31	—	—	—	—
64	P10	P20	P30	—	—	—	—

Fig 3 Biaxial load waveforms and stress ranges

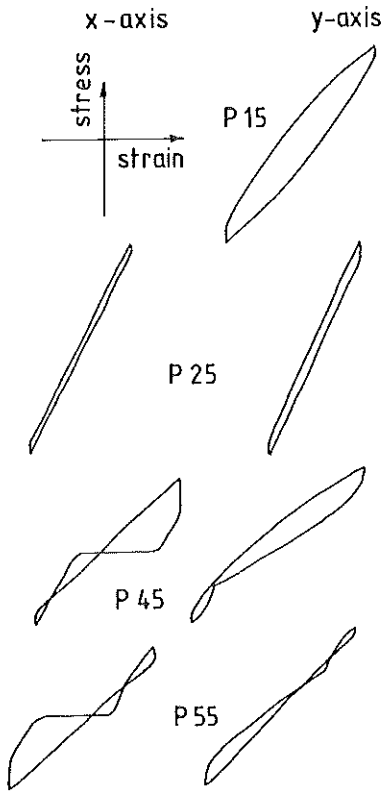

Fig 4 Observed hysteresis loops for tests at 560 MPa stress range in 316 stainless steel

Experimental results

The crack extension results are presented in Fig. 5 in terms of crack growth rate plotted against K, where

$$\Delta K = \Delta\sigma\sqrt{\{\pi a \sec(\pi a/2w)\}} \tag{24}$$

and $\Delta\sigma$ is the stress range normal to the crack, including the compressive portion. The width of the specimen, $2w = 101.9$ mm, has been modified to allow for stiffening of the edges, which affects the K calibration (**14**). Although LEFM analyses are not strictly applicable, equation (24) is used only as a convenient parameter in plotting the results at high stresses, since it provides a suitable correlation factor for the effects of finite plate width.

At a stress level of $\Delta\sigma = 560$ MPa (Fig. 5(a)), specimen P15 subjected to uniaxial loading showed a faster crack growth rate than out-of-phase biaxial specimens P45 and P55 by a factor of approximately 5 and 10, respectively.

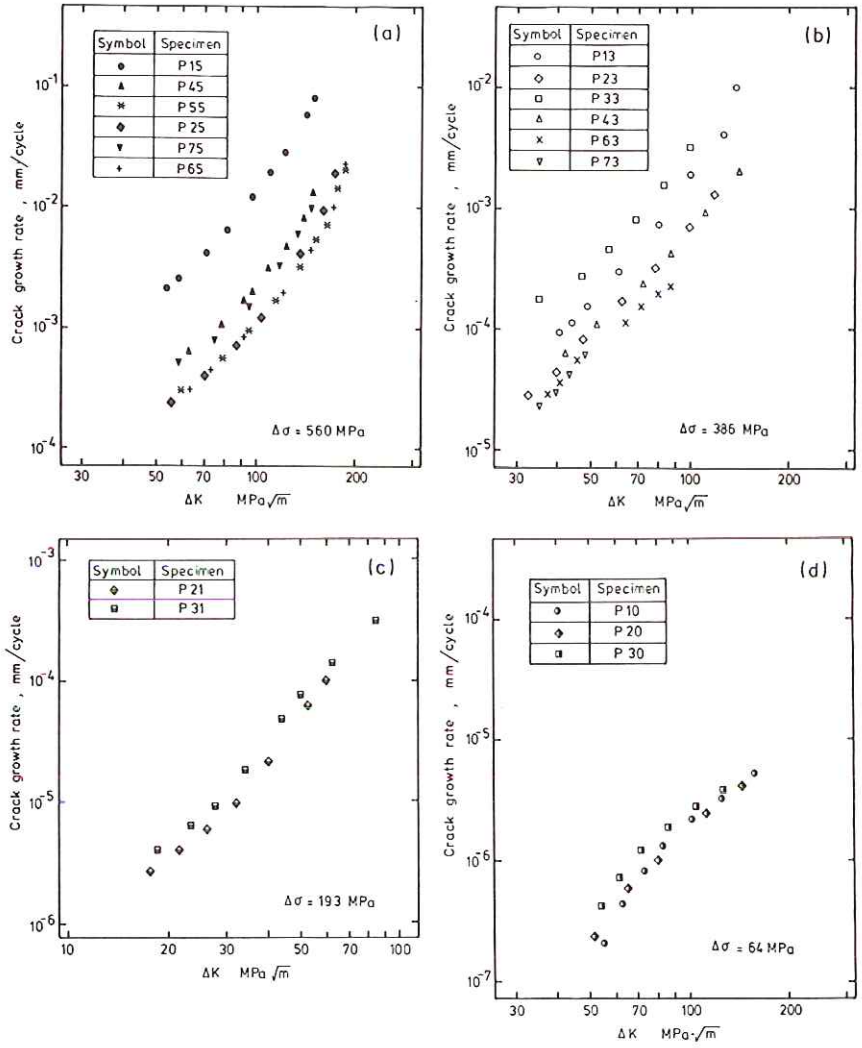

Fig 5 Crack propagation rate as a function of the parameter ΔK (equation (24)), for: (a) $\Delta\sigma =$ 560 MPa; (b) $\Delta\sigma = 386$ MPa; (c) $\Delta\sigma = 193$ MPa; (d) $\Delta\sigma = 64$ MPa

Results for a 90 degree phase difference in equal stress level loaded specimens P75 and P65 were similarly displaced in relation to the uniaxial loading data, i.e., comparable to the results of specimens P45 and P55, respectively. Tests on specimens P55 and P65 ($\phi = +\pi/2$) gave very close results to that for the equibiaxial loaded specimen P25.

For a stress level of $\Delta\sigma = 386$ MPa (Fig. 5(b)), the shear crack gave the fastest crack growth rate (P33), and the results for a 90 degree phase difference (specimens P63 and P73), equibiaxial loading (specimen P23) and out-of-phase biaxial loading (specimen P43) were of a similar nature.

Analysis

From Fig. 5 it is observed that crack growth rates increased as the stress level increased, and so the elastic stress intensity factor K cannot correlate those tests at the highest stress levels for which elastic–plastic conditions are more relevant. It is therefore important to consider whether or not crack growth rates for all biaxial loadings may be predicted by a single theory. The linear elastic stress intensity factor is normally only applied to cases of limited elastic deformation and will not be discussed further in this paper.

Garud (**15**) has used the plastic work per cycle as a measure of damage. It was apparent, however, that the plastic work approach could only be used at high stresses, since at low stress the results appear to diverge (**4**). Indeed, at low stress levels the cyclic stress–strain hysteresis loop will become the elastic line and the plastic work per cycle will be zero, although cracks may still propagate. As mentioned previously, in considering ΔP both the elastic and the plastic strain energy components contribute to crack growth, whereas the hysteresis loop area is only a measure of the plastic work component which will dominate only if $\Delta\varepsilon_p \gg \Delta\varepsilon_e$, as was the case for Garud's data (**15**).

Andrews (**16**) collected data to obtain an in-phase biaxial cyclic stress–strain curve for a 316 type stainless steel (see Fig. 6), which can be described as

$$\tau_{max} = 1161(0.5\gamma_{max})^{0.346} \quad \text{MPa} \tag{25}$$

For 90 degree out-of-phase loading, Lamba and Sidebottom (**17**) indicated that the peak normal stress resulting from out-of-phase hardening of OFHC copper was considerably higher than that for uniaxial cycling, as was also observed by Andrews (**16**). From these results we obtain for the present tests

$$\sigma = 1995\varepsilon_t^{0.346} \quad \text{MPa}$$

or for $\Delta\sigma < 600$ MPa

$$\Delta\sigma = 1190\Delta\varepsilon_p^{0.144} \quad \text{MPa} \tag{26}$$

for in-phase loading, and

$$\sigma = 2523\varepsilon_t^{0.346} \quad \text{MPa}$$

or for $\Delta\sigma < 600$ MPa

$$\Delta\sigma = 1574\Delta\varepsilon_p^{0.144} \quad \text{MPa} \tag{27}$$

The results of all the crack growth experiments in Fig. 5 are assessed in Fig. 7 in terms of ΔP, the elastic–plastic parameter defined by equation (22). The values of X_e and X_p are listed in Table 1 for each case. The plastic term X_p was obtained using equation (26) for proportional loading, but equation (27) where non-proportional cycling was employed. The geometry factor F is given in equation (24). The parameters D and B were taken from ΔP_B (equation (6)) for fully reversed cycling to allow for crack closure, but for repeated tension ($R = 0$) ΔP_c was employed. Three points only are plotted for each test, to avoid undue emphasis being placed on any one experiment.

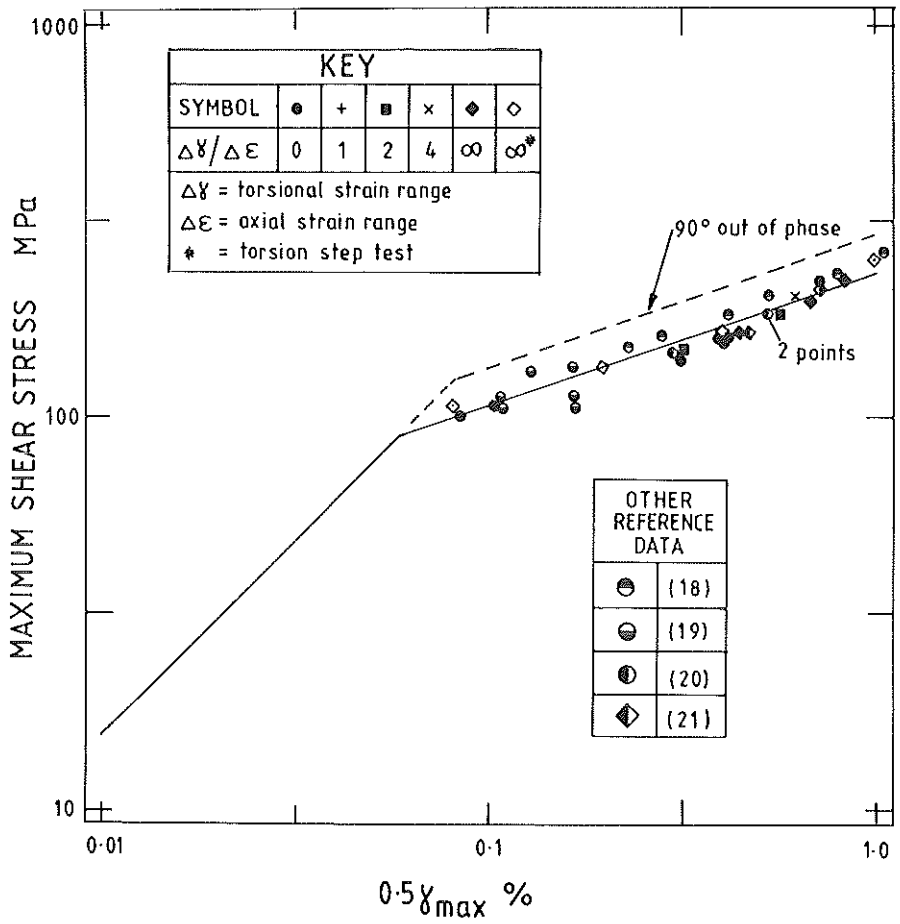

Fig 6 Biaxial cyclic stress strain curve for 316 stainless steel

Discussion

It is found that ΔP provides some correlation in Fig. 7 for all the crack growth results under complex biaxial loadings. The points for uniaxial and shear loads fall on parallel straight lines, except for $\Delta\sigma = 64$ MPa, irrespective of stress level, but the results of equibiaxial load tests show some scatter (although within a factor of ± 3) when compared with the uniaxial test. All out-of-phase results fall within this scatter band. However, the scatter band is reduced to a factor of ± 2 if the results for $\Delta\sigma = 64$ MPa are ignored. Comparison with Fig. 5 shows that a ΔK plot gives scatter of 4 orders of magnitude on crack growth rate, e.g., at ΔK equal to 150 MPa$\sqrt{\text{m}}$ from 10^{-1} to less than 10^{-5} mm/cycle over the stress levels considered here.

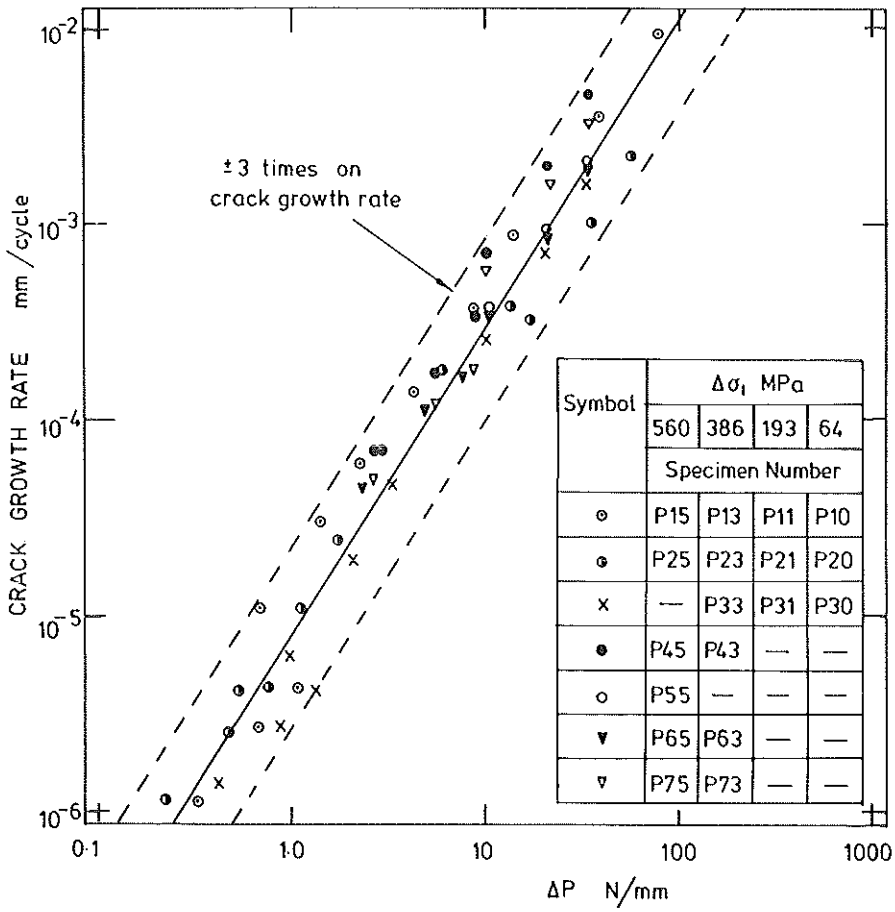

Fig 7 Correlation of all crack propagation tests by the ΔP parameter

The data on Fig. 7 for $da/dN < 5 \times 10^{-6}$ mm/cycle correspond to tests with $\Delta\sigma = 64$ MPa. Therefore, ΔP was determined from equation (7) since $R = 0$. The bad correlation with the tests for fully reversed cycling may be attributed to the simple assumptions involved in the crack closure analysis presented in Appendix 1, and to the close proximity to threshold conditions (see Fig. 5(d)).

The crack growth rate calculations employed in this approach require the corresponding cyclic stress–strain curve derived from a smooth specimen test. This approach may correlate the uniaxial results (when presented in terms of ΔP) with the crack growth rates produced under either in-phase or out-of-phase loads, over a wide range of cyclic stress levels and waveforms at room temperature. Thus, cyclic deformation response plays an important role in

Table 1 Loading parameters

Test No.	*Frequency (Hz)*	$2\sigma_a$ *(MPa)*	$\Delta\sigma_{eff}$ *(MPa)*	$\Delta\varepsilon_p$ $(\times 10^4)$	X_e (N/mm^2)	X_p (N/mm^2)
P15	0.10	560	560	53.3	0.792	2.240
P25	0.10	560	499	23.9	0.629	0.892
P45	0.10	560	560	7.64	0.792	0.320
P55	0.10	560	560	7.64	0.792	0.320
P65	0.10	560	560	7.64	0.792	0.320
P75	0.10	560	560	7.64	0.792	0.320
P13	5.2	383	383	3.81	0.370	0.109
P23	0.94	387.9	345.7	1.87	0.302	0.0484
P33	0.93	385.7	454.7	12.6	0.522	0.426
P43	0.51	383	383	0	0.370	0
P63	0.53	383	383	0	0.370	0
P73	0.52	383	383	0	0.370	0
P11	10	193	193	0	0.094	0
P21	7	191.3	170.5	0	0.073	0
P31	4.1	195.2	230	0	0.134	0
P10	20	66.6	66.6	0	0.011	0
P20	20	62.7	55.9	0	0.0079	0
P30	20	63.1	74.4	0	0.014	0

controlling fatigue crack extension which cannot be ignored in fracture mechanics analyses.

The lack of correlation at low stress range shows that the ΔP correlation parameter needs further developments as do other crack propagation models, for non-proportional loading situations. Note that ΔP fails to conform with LEFM analyses at low stresses and the methods of assessing crack closure could clearly be improved.

Conclusions

(1) A new parameter, ΔP, is proposed for correlating Mode I fatigue crack growth rate for elastic–plastic situations of biaxial stress at both low and high stress levels.
(2) This approach may be applied to both in-phase and out-of-phase biaxial stress cycling if the corresponding cyclic stress–strain curve is used.
(3) The parameter ΔP may be related to the cyclic range of the J integral for uniaxial loading only.

Acknowledgement

H. X. Pei would like to thank The Royal Society of London for its support.

Appendix 1 Derivation of expressions for ΔP

Fully reversed loading with no closure

For the hysteresis loop depicted in Fig. 1, by using the displaced axes $\sigma'\varepsilon'$, the total area under the stress–strain curve is given by

$$W_A = W_e + W_p + W_s = \int_0^{\Delta\varepsilon} \sigma' \, d\varepsilon'$$

For the assumed hysteresis loop shape

$$\varepsilon' = \sigma'/E + 2(\sigma'/2A)^{1/\alpha}$$

hence

$$d\varepsilon' = d\sigma'/E + (\sigma'/2A)^{1/\alpha - 1} \, d\sigma'/A\alpha$$

Integrating between limits of 0 to $\Delta\sigma$ for σ'

$$W_A = \Delta\sigma^2/2E + 2\Delta\sigma(\Delta\sigma/2A)^{1/\alpha}/(1 + \alpha) = \Delta\sigma^2/2E + \Delta\sigma\Delta\varepsilon_p/(1 + \alpha)$$

where

$$W_e = \Delta\sigma^2/2E$$
$$W_p + W_s = \Delta\sigma \cdot \Delta\varepsilon_p/(1 + \alpha)$$

From equation (4), a value of ΔP may be derived

$$\Delta P_A = 2\pi F^2 a(W_e + W_p + W_s) \tag{28}$$

Fully reversed loading with closure at zero stress

If the crack is assumed to open at zero load, ΔP can be estimated from the upper half of the hysteresis loop in Fig. 1. Thus the area under the loop

$$\begin{aligned} W_B &= \int_{\varepsilon_e}^{\Delta\varepsilon} (\sigma' - \Delta\sigma/2) \, d\varepsilon' \\ &= \int_{\Delta\sigma/2}^{\Delta\sigma} (\sigma' - \Delta\sigma/2)(d\sigma'/E + (\sigma'/2A)^{1/\alpha - 1} \, d\sigma'/A\alpha) \\ &= \Delta\sigma^2/8E + \Delta\sigma \cdot \Delta\varepsilon_p\{(1 - \alpha) + \alpha/2^{1/\alpha}\}/\{2(1 + \alpha)\} \end{aligned}$$

The term $\alpha/2^{1/\alpha}$ may be neglected since for most engineering metals $0.1 \leq \alpha \leq 0.2$ so that

$$0.00011 \leq \alpha/\{2^{1/\alpha}(1 - \alpha)\} \leq 0.0078$$

Thus

$$W_B = \Delta\sigma^2/8E + \Delta\sigma\Delta\varepsilon_p(1 - \alpha)/\{2(1 + \alpha)\}$$

and in Fig. 1

$$W_p = \Delta\sigma \cdot \Delta\varepsilon_p(1 - \alpha)/(1 + \alpha)$$

From equation (4), a value of ΔP may be derived

$$\Delta P_B = 2\pi F^2 a(W_e + 2W_p)/4 \tag{6}$$

which may be compared to the previous solution, written as

$$\Delta P_A = 2\pi F^2 a\{W_e + W_p/(1 - \alpha)\} \tag{5}$$

since

$$W_S = \Delta\sigma\Delta\varepsilon_p\alpha/(1 + \alpha)$$

Repeated load cycling with no closure (R = *0)*

If any strain ratchetting effects can be neglected, the solution in this case will correspond to ΔP_A, noting that no shift will arise between the axes σ, ε and σ', ε' in Fig. 1.

References

(1) BROWN, M. W. and MILLER, K. J. (1982) Two decades of progress in the assessment of multiaxial low cycle fatigue, in *Low-cycle fatigue and life prediction, ASTM STP 770*, ASTM, Philadelphia, PA, pp. 482–499.

(2) GARUD, Y. S. (1981) Multiaxial fatigue: a survey of the state of the art, *J. Testing Evaluation*, **9**, 165–178.

(3) KANAZAWA, W., MILLER, K. J., and BROWN, M. W. (1977) Low-cycle fatigue under out-of-phase loading conditions, *J. Engng Mater. Technol.*, **99**, 222–228.

(4) JORDAN, E. H., BROWN, M. W., and MILLER, K. J. (1985) Fatigue under severe non-proportional loading, in *Multiaxial fatigue, ASTMP STP 853*, ASTM, Philadelphia, PA, pp. 569–585.

(5) DOWLING, N. E. (1977) Crack growth during low-cycle fatigue of smooth axial specimens, in *Cyclic stress–strain and plastic deformation aspects of fatigue crack growth, ASTM STP 635*, ASTM, Philadelphia, PA, pp. 97–121.

(6) STARKEY, M. S. and SKELTON, R. P. (1982) A comparison of the strain intensity and cyclic *J* approaches to crack growth, *Fatigue Engng Mater. Structures*, **5**, 329–341.

(7) TOMKINS, B. (1984) High strain fatigue, in *Subcritical crack growth due to fatigue, stress corrosion, and creep* (Edited by LARSSON, L. H.), Elsevier, New York, pp. 239–266.

(8) BROWN, M. W., LIU, H. W., KFOURI, A. P., and MILLER, K. J. (1980) An analysis of fatigue crack growth under yielding conditions, in *Advances in fracture research* (Edited by FRANCOIS, D.), Pergamon Press, Oxford, Vol. 2, pp. 891–898.

(9) BROWN, M. W., DE LOS RIOS, E. R., and MILLER, K. J. (1984) A critical comparison of proposed parameters for high strain fatigue crack growth, presented at ASTM Symposium on Fundamental Questions and Critical Experiments in Fatigue, Dallas, TX, USA.

(10) CAI, Q. (1977) Crack analysis in high strain field, *Acta Met. Sinica*, **13** (in Chinese).

(11) DOWLING, N. E. (1978) Stress–strain analysis of cyclic plastic bending and torsion, *J. Engng Mater. Technol.*, **100**, 157–163.

(12) ABDEL-RAOUF, H., TOPPER, T. H., and PLUMTREE, A. (1977) Cyclic plasticity and Masing behaviour in metals and alloys, in *Fracture* (Edited by TAPLIN, D. M. R.), Pergamon Press, Oxford, Vol. 2, pp. 1207–1215.

(13) HOPPER, C. D. and MILLER, K. J. (1977) Fatigue crack propagation in biaxial stress fields, *J. Strain Analysis*, **12**, 23–28.

(14) BROWN, M. W. and MILLER, K. J. (1985) Mode I fatigue crack growth under biaxial stress at room and elevated temperatures, in *Multiaxial fatigue, ASTM STP 853*, ASTM, Philadelphia, PA, pp. 135–152.

(15) GARUD, Y. S. (1981) A new approach to the evaluation of fatigue under multiaxial loadings, *J. Engng Mater. Technol.*, **103**, 118–125.

(16) ANDREWS, R. M. (1986) *High temperature fatigue of AISI 316 stainless steel under complex biaxial loading*, PhD thesis, University of Sheffield, UK.

(17) LAMBA, H. S. and SIDEBOTTOM, O. M. (1978) Cyclic plasticity for non-proportional paths: Path 1 – Cyclic hardening, erasure of memory, and subsequent strain hardening experiments, *J. Engng Mater. Technol.*, **100**, 96–111.

(18) National Research Institute for Metals (1979) Elevated temperature high cycle and low cycle fatigue properties of SUS 316-HP hot rolled stainless steel plate, Fatigue Data Sheet 15, NRIM, Japan.

(19) JASKE, C. E. and FREY, N. D. (1982) Long life fatigue of Type 316 stainless steel at temperatures up to 593°C, *J. Engng Mater. Technol.*, **104**, 137–144.

(20) JACQUELIN, B., HOURLIER, F., and PINEAU, A. (1983) Crack initiation under low cycle multiaxial fatigue in Type 316L stainless steel, *J. Pressure Vessel Technol.*, **105**, 138–143.

(21) JACQUELIN, B., HOURLIER, F., and PINEAU, A. (1985) Crack initiation under low cycle multiaxial fatigue, *Multiaxial fatigue, ASTM STP 853*, ASTM, Philadelphia, PA, pp. 285–313.